Progress In Electromagnetics Research M, Vol. 66, 53–63, 2018

Design of Compact Wideband Serpentine Patch Antenna for Ingestible Endoscopic Applications

Shikha Sukhija*, Rakesh K. Sarin, and Nitesh Kashyap

Abstract—A miniaturized serpentine patch antenna is presented for Industrial, Scientific and Medical band (2.4–2.48 GHz) applications. The proposed antenna is fabricated on a Rogers RT/duroid5880 substrate having permittivity of 2.2 and loss tangent of 0.0009. In comparison with other traditional structures, this antenna has an electrical length of 0.961λ with 29.2% impedance bandwidth which is advantageous for higher data rate transmission. In order to test the performance, the proposed antenna is tested in a silicone feeding tube. The simulated and measured results show good agreement with each other. Defected ground structure is also incorporated to enhance the performance of the proposed structure. All the simulations have been carried out on FDTD based Empire XCcel tool.

1. INTRODUCTION

In recent years, wireless technologies have received much attention for their use in biomedical applications. For communication between implanted circuitry in a patient and base station, antenna acts as an important element in a telemetry system. Nowadays microstrip patch antenna plays a vital role for these applications due to its profitable properties and advantageous qualities such as compactness, light weight, ease of fabrication, economical efficiency and many others. These antennas can be used for implantable/ingestible as well as remote health monitoring systems in which physiological data of a patient can be monitored at home, such as pressure monitoring, glucose monitoring, and temperature monitoring [1–4], avoiding longer stays and regular checkup in hospitals. So, for a telemetry system, one of the two antennas should be outside the human body for the purpose of communication.

Since miniaturization is the basic need for the use of these devices in biomedical applications, one has to consider the main constraint of miniaturization so that the designed antenna can be easily implanted/ingested in a human body. Several types of techniques are adopted in literature to achieve miniaturization such as meandered structures, slots, PIFA, shorting pin, use of metamaterials and high permittivity substrates [5–9].

After incorporating miniaturizing techniques, one should emphasize bandwidth enhancement so that higher data rate transmission can be achieved. Further, if there is shift in frequency due to surrounding environment, the antenna will still be within that bandwidth. So, a wide-band antenna is required for video based data transmission. It can be possible within larger bandwidth only. In such situations, some structures can be taken into consideration such as defected ground structures [10], metamaterials [11–13] and frequency selective surfaces [14] for the enhancement of bandwidth of an antenna. Some frequency bands are allocated for an antenna to be used in biomedical applications such as MICS and ISM band. MICS operates in 402–405 MHz band [15], and frequencies allowed for ISM band are 27 MHz, 433 MHz and 2.45 GHz [16].

Received 1 December 2017, Accepted 7 March 2018, Scheduled 22 March 2018

* Corresponding author: Shikha Sukhija (shikhasukhija@yahoo.co.in).

The authors are with the Department of Electronics & Communication, National Institute of Technology, Jalandhar, Punjab 144011, India.

In this paper, a serpentine microstrip patch antenna with and without a defected ground structure is presented and discussed. This antenna can be used in gastrostomy feeding tube for the purpose of endoscopy so that the internal condition of the patient can be examined through the communication between internal antenna and base station outside the human body. As the diameter of feeding pipe varies from 2.64 mm to 9.9 mm [17], the antenna and electronic circuitry must be of the size to fit in the dimensions. It is worth to note that commercial mini-cameras [18] and rechargeable batteries [19] having dimensions about 5 mm have been developed and can be easily incorporated in the feeding tube and/or capsule structure.

2. ANTENNA DESIGN SPECIFICATIONS

In this paper, a serpentine microstrip patch antenna with dimensions of $L \times W\,\text{mm}^2$ is proposed. This proposed antenna is fabricated on a Rogers RT/Duroid 5880 substrate with dielectric constant (ε_r) of 2.2 and loss tangent ($\tan\delta$) of 0.0009. The width of the proposed antenna is chosen so as to fit in the size of the silicon tube [17]. The thickness of the substrate is taken as 0.78 mm. Fig. 1 shows the top view of the proposed antenna. Regular serpentine structure is used with gap G in consecutive slots. The reason for incorporating this structure is to increase the current path and minimize the size of antenna. Further, to enhance the bandwidth and reduce the size of the design, regular sots with uniform gap of $G = 2$ mm is cut in radiating patch. To obtain the required performance parameters of the proposed design, the optimized dimensions are used in Fig. 1. For better understanding, Fig. 1(a) shows the overall antenna design. Fig. 1(b) shows the zoomed upper view of the radiating patch, and Fig. 1(c) shows the zoomed lower view of the antenna. Table 1 presents all the optimized dimensions and their values for the proposed antenna. S is the width of serpentine structure. Partial ground plane is designed on back side of the substrate with dimensions of $L_G \times W_G$. P1E is the position of the wave port situated at the edge of feed line [20]. The optimization was supported by fine tuning of all the dimensions using FDTD based Empire XCcel simulator [20].

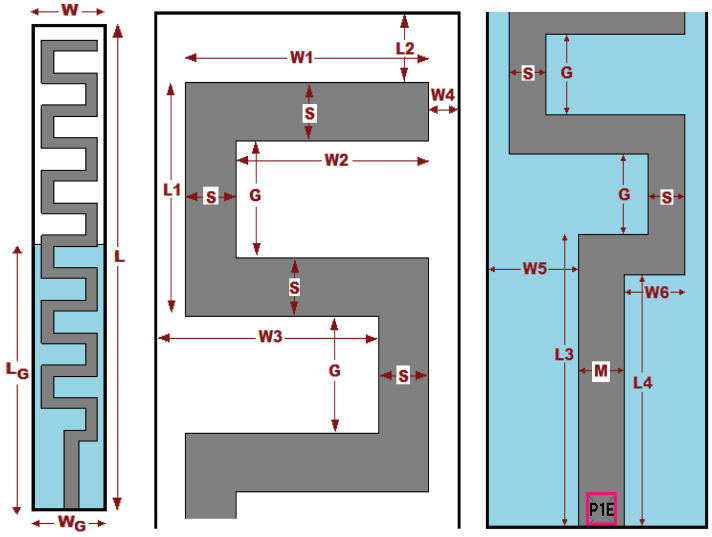

Figure 1. (a) Proposed antenna (b) zoomed view of the upper patch and (c) zoomed view of the lower design.

In addition, a defected ground structure is also included in the proposed antenna. Usually, a defected ground structure is placed below the microstrip line, and it disturbs the electromagnetic field near the defect. This surrounding electric field generates capacitive effect (C) whereas the current near the defect gives rise to inductive effect (L). Fig. 2 illustrates the presented antenna with an inverted defected ground structure in which the defect is the same as the serpentine structure on the ground

Table 1. Parameters and their values in mm.

Dimensions	Values in mm	Dimensions	Values in mm
L	44.50	**W**	6.00
L1	4.00	**W1**	4.80
L2	1.20	**W2**	3.80
L3	7.30	**W3**	4.40
L4	6.30	**W4**	0.60
L_G	24.50	**W5**	2.50
G	2.00	**W6**	1.65
M	1.25	**W_G**	6.00

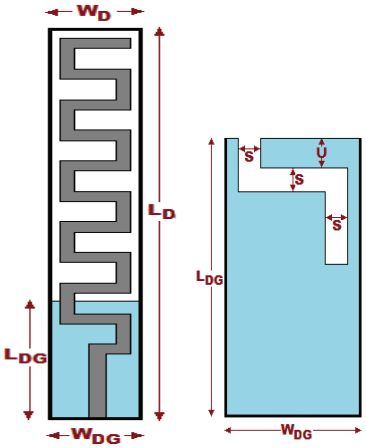

(a) (b)

Figure 2. (a) Proposed antenna with DGS and (b) Design of defected ground structure.

Dimensions	Values in mm
W_D	6.00
L_D	38.10
W_{DG}	6.00
L_{DG}	11.50
S	1.0
U	1.20

Table 2. Parameters and their values in mm for the proposed antenna with defected ground structure.

plane. To enhance the performance of the antenna, a defected ground structure is used in this design. By using this inverted DGS structure, the overall antenna size and ground size are reduced to $L_D \times W_D$ and $L_{DG} \times W_{DG}$, respectively. The parameters and their values in mm are presented in Table 2 where the same spacing S is also used for the defected ground structure.

3. PARAMETRIC VARIATIONS

3.1. Varying Number of Turns

For designing a patch antenna with reduced size, meandering of the patch is an important technique for such kind of antenna realization. Meandering of the patch lengthens the current path which in turn lowers the resonant frequency. Taking this into consideration, the proposed antenna is designed by adding number of turns consecutively to the patch. Through this progression, the optimization of the proposed serpentine structure is succeeded for required performance, and this has become the most prominent feature for the antenna design and parametric study. Fig. 3 shows the variation of S_{11} characteristics with respect to frequency for various number of turns denoted by N. It can be observed that as the number of turn increases, the frequency shifts to lower value of the graph. As the number of turns increases from $N = 4$ to $N = 16$, the resonant frequency shifts from 2.64 GHz to 2.40 GHz, and S_{11} parameter shifts from -25.26 dB to -23.86 dB. For $N = 12$, the performance gives rise to an antenna with center frequency 2.48 GHz and S_{11} parameter -40.26 dB. The impedance graph in Fig. 4

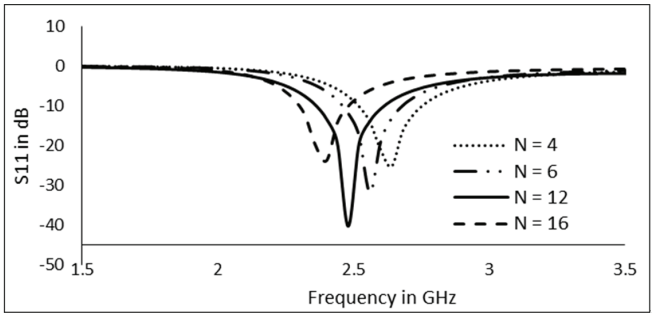

Figure 3. Simulated S_{11} plot showing effect of N.

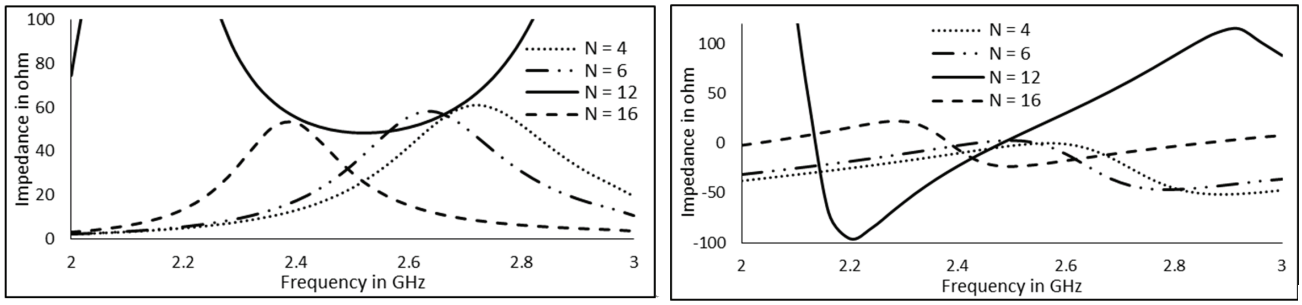

Figure 4. Simulated plots (a) frequency vs. impedance (real-part) and (b) frequency vs. impedance (imaginary part).

shows that the obtained characteristic impedance for twelve turns is closer to 50 Ω and 0 Ω for real value and imaginary value, respectively.

3.2. Ground Plane Length Variation (L_G)

Length of the ground plane in patch antenna designing is a very important factor for determining the antenna performance. Fig. 5 shows the parametric variation of the ground plane length L_G in respect of S_{11} parameter. By varying L_G from partial ground to full ground, the peak value of S_{11} shifts towards higher frequencies. It can be seen from the graph of S_{11} parameter vs. frequency that as the value of ground plane length increases from 11.5 mm to 44.5 mm the antenna resonant frequency shifts from 2 GHz to 3 GHz while in case of full ground plane ($L_G = 44.5$ mm), the resonant frequency diminishes in the frequency range of 1 GHz to 5 GHz. On the other hand, the S_{11} parameter increases

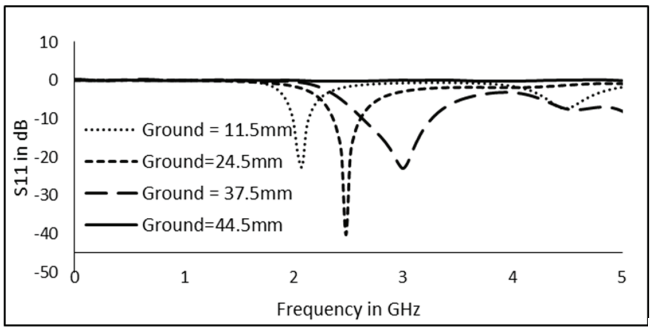

Figure 5. Simulated S_{11} plot showing effect of L_G.

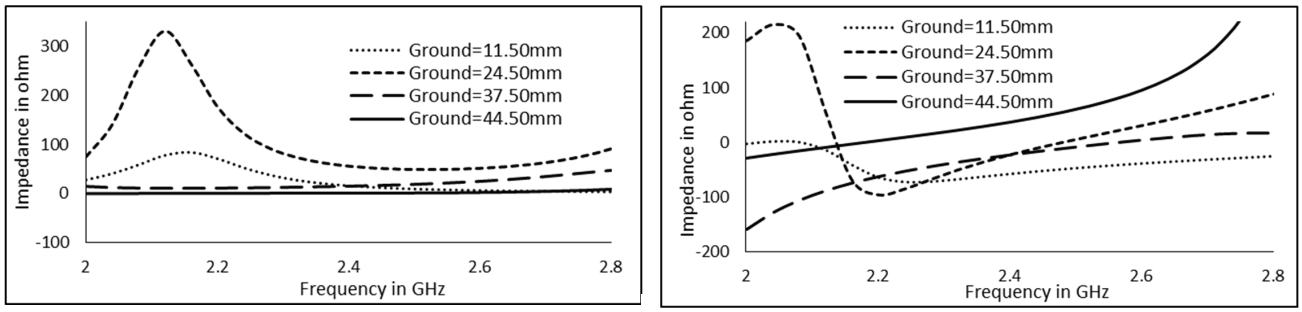

Figure 6. Simulated plots (a) frequency vs. Impedance (real-part) and (b) frequency vs. impedance (imaginary part).

from −22.48 dB to −40.26 dB for 2.08 GHz to 2.48 GHz frequency, and then it decreases to −22.89 dB at 3 GHz frequency. So, it can be concluded that increase in L_G reduces the effective size of the antenna which leads to the frequency shift to the right side. Fig. 6 shows the graph of impedance with respect to frequency which shows that for optimized ground plane at 24.5 mm, the real value of impedance varies over the frequencies above and below 2.48 GHz. As the ground plane length is optimized to 24.5 mm, the real value for impedance moves nearer to 50 Ω, and imaginary value of impedance moves toward 0 Ω.

3.3. Varying Length L4

Length L4 is the gap between the serpentine patch and the substrate boundary as shown earlier in Fig. 1(c). This length variation actually indicates the shifting of serpentine structure. For the purpose of parametric study the value of L4 is varied from 3.30 mm to 7.30 mm in steps of 1 mm. Fig. 7 shows the graph of S_{11} parameter vs. frequency for different values of L4 keeping all other parameters fixed. It can be concluded that as L4 increases from 3.3 mm to 6.3 mm, the value of S_{11} parameter increases from −26.68 dB to −40.36 dB, and center frequency decreases from 2.67 GHz to 2.48 GHz. And again increase in the value of this length from 6.3 mm to 7.3 mm leads to the decrease in the value of S_{11} parameter from −40.36 dB to −27.06 dB, and center frequency shifts from 2.48 GHz to 3.38 GHz. This is because the length of the serpentine structure is fixed, and only L4 is varied which does not effectively shift the frequency to the left side. Further increase in the length of L4 results in the increased size of the proposed antenna which is not required.

So, the optimized value of L4 for the proposed structure is obtained as 6.30 mm. On the other hand, as length L4 is optimized to 6.30 mm, the graph of impedance vs. frequency in Fig. 8 shows that the real value of impedance approaches 50 Ω and that imaginary value of impedance comes close to 0.

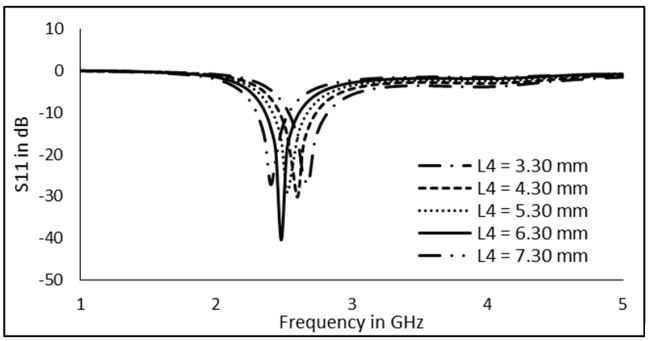

Figure 7. Simulated S_{11} plot showing effect of varying L4.

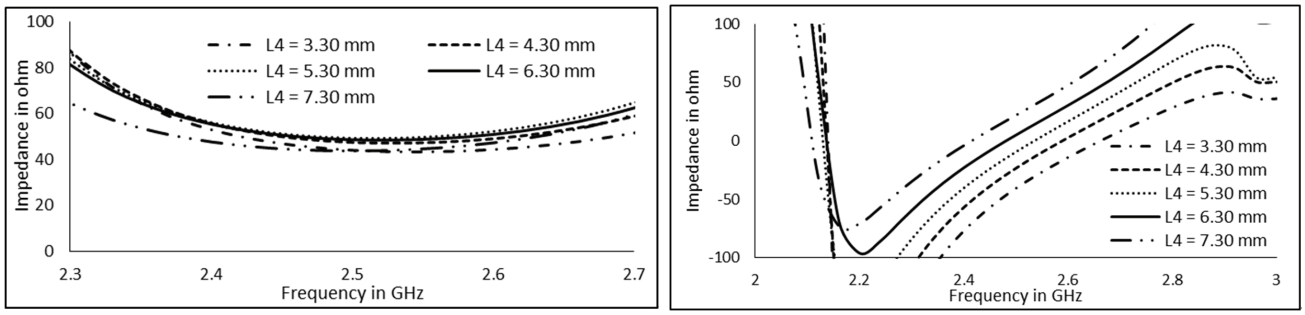

Figure 8. Simulated Impedance vs. Frequency plot. (a) Frequency vs. impedance (real part) and (b) Frequency vs. impedance (imaginary part).

4. RESULTS AND DISCUSSION

4.1. Simulation and Measurement

The performance of the proposed antenna structure is analyzed in terms of S_{11} parameter. SMA connector of the antenna to be tested is connected to coaxial cable of vector network analyzer. One port calibration is performed using calibration standards such as short, open and load. The graph of S_{11} parameter vs. frequency is plotted for the proposed antenna as simulated by Finite Difference Time Domain (FDTD) based Empire XCcel simulator together with measurement using VNA. The serpentine patch antenna is fabricated and tested. The front and back views of the fabricated antennas are shown in Fig. 9.

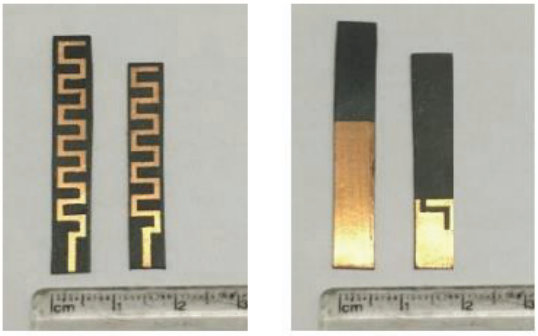

Figure 9. Images of fabricated antennas (a) front view and (b) back view.

The performance of the proposed antenna is also presented with the effect of using defected ground structure. Through the number of simulations as discussed in the last section, Fig. 10 illustrates the optimized simulation and measurement results for serpentine antenna with and without defected ground plane. The graph displays S_{11} parameter variation with respect to frequency. It can be illustrated that the proposed antenna structure exhibits -10 dB simulated bandwidth of 270 MHz, while using DGS it exhibits the simulated bandwidth of 668 MHz. Besides this, the center frequencies obtained are 2.39 GHz and 2.48 GHz for antenna with and without DGS, respectively, which implies that the proposed antenna can be used for earlier stated ISM band applications. The simulated and measured results show good similarity within the frequency range.

In order to verify that the proposed structure can be used for ingestible applications, the performance is analyzed by inserting the antenna in a silicone tube. Due to its good biocompatibility

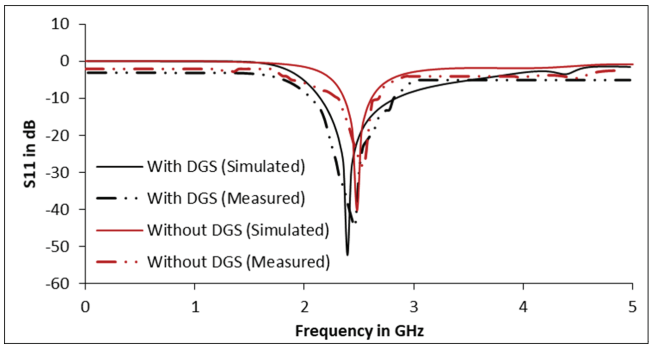

Figure 10. Simulated and measured S_{11} performance for antenna with and without DGS.

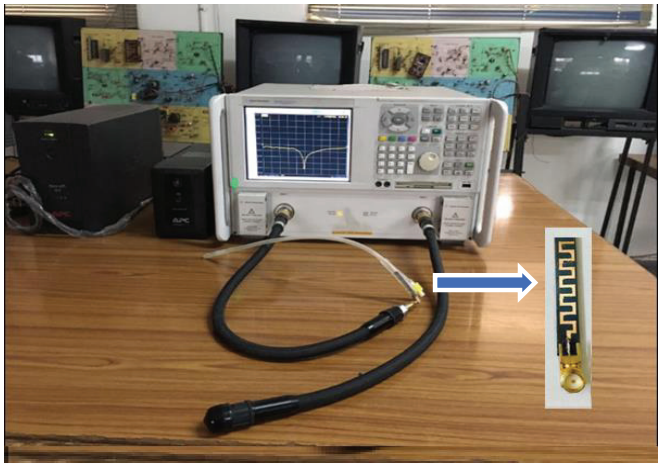

Figure 11. Measurement in silicone feeding tube using VNA.

nature and long term implant property, silicone is widely used in catheters. Different types of feeding tubes could be taken into consideration for the patient as per the requirement, and a tube, named as PEG (Percutaneous Endoscopic Gastrostomy), is inserted into the stomach of the patient to supply the essential nutrition [17, 21]. The diameter of the tube is taken as 20F (i.e., 6.66 mm) [17]. So the proposed antenna is able to fit in the tube. The measurement results are obtained through the experiment of the proposed antenna in the PEG feeding tube using vector network analyzer displayed in Fig. 11. The figure implies that with the use of DGS, the performance of the proposed antenna is still within the range of frequency of interest due to enhanced bandwidth. As data rate is directly proportional to bandwidth in digital communication, wideband is the only requirement to transmit sufficient image resolution and higher data rate.

By incorporating pipe, the surrounding environment for the antenna gets changed leading to the frequency shift from its original value but still within that frequency range because of antenna's wideband characteristics. It can be illustrated that the antenna without DGS resonates at 2.52 GHz and exhibits 199 MHz simulation bandwidth in the feeding tube while the antenna with DGS resonates at 2.53 GHz frequency and has simulation bandwidth of 483 MHz as represented in Fig. 12.

It can be seen that the proposed serpentine antenna measurement in silicone tube shows good agreement with the simulated results in silicone pipe, which demonstrates that the designed antenna can be realized for ingestible applications. To compare and evaluate the characteristics of the antenna, the simulated and measured S_{11} parameters, resonant frequencies, bandwidths, impedances and VSWRs are described in Table 3.

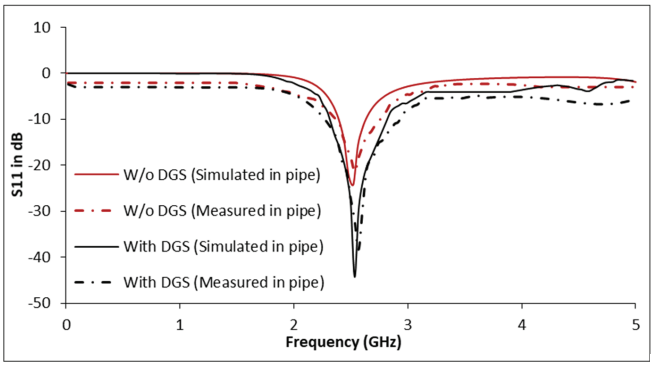

Figure 12. Simulated and measured S_{11} performance for antenna with and without DGS in silicone pipe.

Table 3. Comparison of simulated and measured results.

Antenna	Simulation/ Measurement	Frequency (GHz)	S_{11} (dB)	Bandwidth (MHz)	VSWR	Impedance (Ω)
Antenna with DGS	Simulated	2.39	−52.30	668	1.005	50.22
	Measured	2.46	−44.30	762	1.012	-
Antenna without DGS	Simulated	2.48	−40.25	270	1.020	49.03
	Measured	2.54	−28.45	320	1.079	-
Antenna with DGS in pipe	Simulated	2.53	−44.30	483	1.012	52.65
	Measured	2.57	−38.25	621	1.025	-
Antenna without DGS in pipe	Simulated	2.52	−24.20	199	1.131	51.88
	Measured	2.53	−21.33	348	1.188	-

4.2. Current Distribution

The current distribution for the proposed antenna is presented in Fig. 13. It can be visualized from Fig. 13(a) that the current flows uniformly over the patch and is intensive in the serpentine structure of the antenna. However, the flow of current in horizontal strips of the serpentine patch is in opposite direction which results in very low or negligible radiation. In the case of vertical strips, the flow of current is in unified direction as symbolized by circles in Figure 13. So, it can be concluded that current is an eminent source of radiation for the proposed antenna.

The simulated current distribution of the proposed antenna at different frequencies of its bandwidth is presented in Figs. 13(b), (c) and (d). The current at lower frequency is generated because of the edges of the patch. Lower, upper and resonant frequencies f are calculated by following equations [22]

$$T_o = T_1 + T_2 + T_3 + T_4 + T_5 \tag{1}$$

$$f = \frac{c}{T_o\sqrt{\varepsilon_r}} \tag{2}$$

where T_o is the total length which contributes to the flow of current. With the help of above relations, the calculated lower, upper and operating frequencies are obtained as 2.251 GHz, 2.869 GHz and 2.502 GHz, respectively.

4.3. Radiation Patterns

The omnidirectional radiation pattern is an essential requirement for an ingestible antenna due to its random placement. The radiation patterns of the proposed antenna with and without DGS are illustrated in Fig. 14. All the patterns are plotted at 2.4 GHz frequency. These radiation pattern

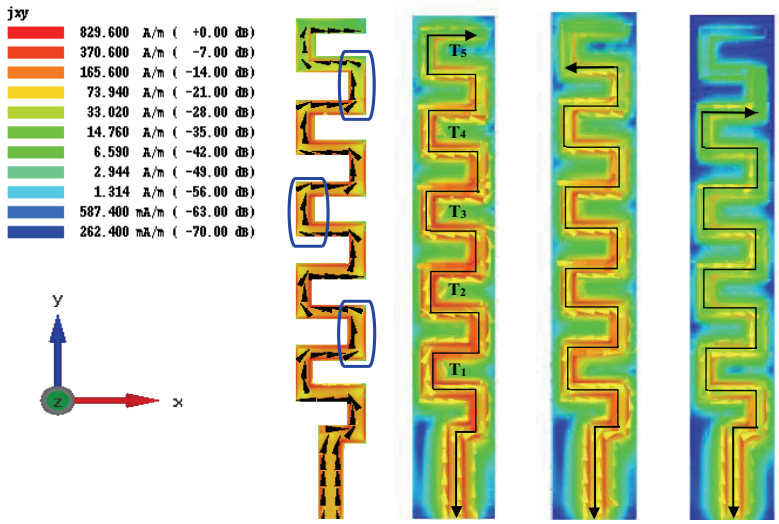

Figure 13. Simulated current distribution, (a) arrow plot, (b) at 2.14 GHz, (c) at 2.39 GHz and (d) at 2.81 GHz.

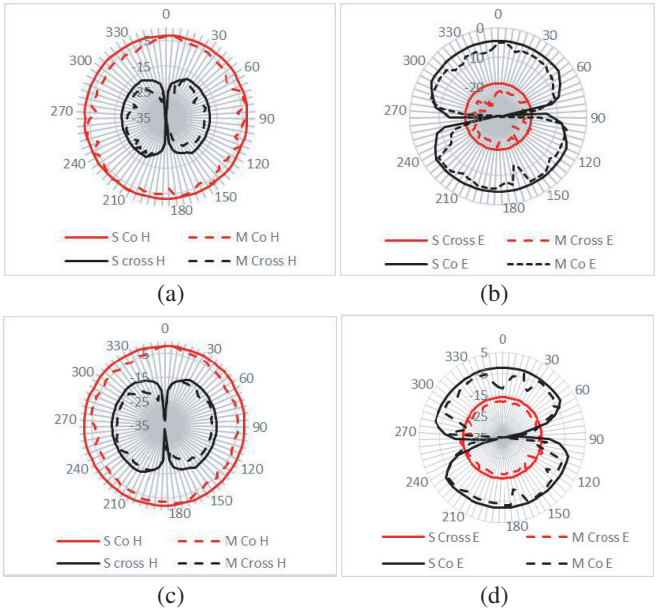

Figure 14. Simulated and measured radiation patterns for antenna without DGS at 2.4 GHz. (a) H-plane, (b) E-plane and antenna with DGS, (c) H-plane, (d) E-plane.

measurements for RF and microwave range frequencies are performed using an anechoic chamber. The figure shows the radiation patterns for both E-plane and H-plane. For H-plane, the co-polar component shows monotonous behavior as expected, and the measured patterns also show similar characteristics except at some points owing to the existence of parasitic effect in SMA connector. In contrast, the measured cross polarization is about -39 dB, and simulated one is about -37 dB for antenna without DGS. For the antenna with DGS, the measured cross polarization is around -34 dB, and simulated one is about -32 dB shown in Figs. 14(a) and 14(c), respectively. On the other hand, the co-polar component in E-plane has a well-known shape like figure eight (8) as expected. Measured results

show good resemblance with simulated ones. Some deviation occurs due to the SMA connector and feeding connector, but these are still within the acceptable limits. Measured cross polarization is near −18 dB, and calculated one is almost −22 dB for antenna without DGS. For the antenna with DGS, simulated value is about −15 dB, and measured one is almost −19 dB as shown in Figs. 14(b) and 14(d), respectively.

4.4. Gain and Efficiency

It can be illustrated from Fig. 15 that the obtained gain of the proposed antenna is 0.991 dB at the operational frequency of 2.4 GHz. On the other hand, the efficiency obtained for the proposed serpentine antenna is approximately 96% at the design frequency, which is shown in Fig. 16.

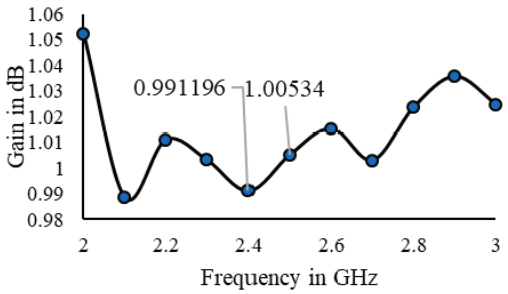

Figure 15. Simulated gain vs. frequency plot.

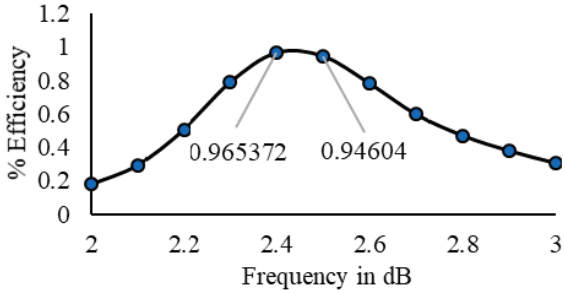

Figure 16. Simulated efficiency vs. frequency plot.

5. CONCLUSION

This paper reports a serpentine patch antenna design for operation in ISM band and explains the comparison between experimental results of proposed antenna with and without a defected ground structure in a silicone tube. With low permittivity substrate, the proposed antenna has small size owing to meandering of radiating patch. A defected ground structure is used to enhance bandwidth for higher data transmission. Isotropic radiation pattern is obtained to transmit signals independent of the antenna position in the pipe. Similar trends of measurement and simulation validate the appealing feature of the proposed serpentine antenna. The characterization and measurement related with the effect of electronic circuitry on antenna performance will be of great interest. The future scope also includes more reduction in size of the antenna so that it can be used in narrow esophagus feeding tubes or varicose veins.

ACKNOWLEDGMENT

The authors would like to thank CARE Lab at Indian Institute of Technology, Delhi for measurement of radiation patterns.

REFERENCES

1. Furse, C. M., "Design of an antenna for pacemaker communication," *Microwaves RF*, Vol. 39, No. 3, 73–76, Mar. 2000.
2. Beach, R. D., F. V. Kuster, and F. Moussy, "Subminiature implantable potentiostat and modified commercial telemetry device for remote glucose monitoring," *IEEE Trans. Instr. Meas.*, Vol. 48, No. 6, 1239–1245, Dec. 1999.
3. Beach, R. D., R. W. Conlan, M. C. Godwin, and F. Moussy, "Towards a miniature implantable in vivo telemetry monitoring system dynamically configurable as a potentiostat or galvanostat for two- and three electrode biosensors," *IEEE Trans. Instr. Meas.*, Vol. 54, No. 1, 61–72, Feb. 2005.

4. Hall, P. S. and Y. Hao, *Antennas and Propagation for Body-Centric Wireless Communications*, Artech House, Norwood, MA, 2006.
5. Kiourti, A. and K. S. Nikita, "A review of implantable patch antennas for biomedical telemetry: challenges and solutions," *IEEE Antennas and Propag. Magazine*, Vol. 54, No. 3, 210–228, Jun. 2012.
6. Sukhija, S. and R. K. Sarin, "Low-profile patch antennas for biomedical and wireless applications," *J. Comput. Electron.*, Vol. 16, No. 2, 354–368, Jun. 2017.
7. Sukhija, S. and R. K. Sarin, "Design and performance of two-sleeve low profile antenna for biomedical applications," *Journal of Electrical Systems and Information Technology*, Vol. 4, No. 1, 49–61, 2017.
8. Sukhija, S. and R. K. Sarin, "A u-shaped meandered slot antenna for biomedical applications," *Progress In Electromagnetics Research M*, Vol. 62, 65–77, 2017.
9. Triple-band metamaterial-inspired antenna using FDTD technique for WLAN/WiMAX applications, *Int. Journal of RF and Computer Aided Engineering*, Vol. 25, No. 8, 688–695, 2015.
10. Kandwal, A., R. Sharma, and S. K. Khah, "Bandwidth enhancement using Z-shaped defected ground structure for a microstrip antenna," *Microwave and Optical Technology Letters*, Vol. 55, 2251–2254, 2013.
11. Islam, M. M., et al., "Compact metamaterial antenna for UWB applications," *Electronics Letters*, Vol. 51, No. 18, 1222–1224, 2015.
12. Sharma, S. K., et al., "Epsilon negative CPW-fed zeroth-order resonating antenna with backed ground plane for extended bandwidth and miniaturization," *IEEE Trans. on Antennas and Propag.*, Vol. 63, No. 11, 5197–5203, 2015.
13. Xiong, H., J.-S. Hong, and Y.-H. Peng, "Impedance bandwidth and gain improvement for microstrip antenna using metamaterials," *Radio Engineering*, Vol. 21, No. 4, 993–998, Dec. 2012
14. Barbagallo, S., A. Monorchio, and G. Manara, "Small periodicity FSS screens with enhanced bandwidth performance," *Electronics Letters*, Vol. 42, No. 7, 7–8, Mar. 2006.
15. Medical implant Communication Service (MICS) federal register, Rules reg., Vol. 64, No. 240, Dec. 1999.
16. Smith, E. K., Radiowave Propagation in ITU-R," *IEEE Magazine in Antennas and Propagation*, Vol. 41, No. 1, 118–119, Feb. 1999.
17. ASGE Technology Committee, R. S. Kwon, S. Banerjee, D. Desilets, et al., "American Society for Gastrointestinal Endoscopy, Technology status evaluation report: enteral nutrition access devices," *Gastrointest Endosc*, Vol. 72, 236-48, 2010.
18. VD6725, STMicroelectronics, Geneva, Switzerland, Jan. 2012.
19. Small Battery Company, Hearing aid batteries, [Online], 2012, Available: http://www.smallbattery.company.org.uk/hearing_aid_batteries.htm.
20. "User and reference manual for the 3D EM time domain simulator empire XCcel," ver.5, IMST GmbH, [Online], 2012, Available: http://www.empire.de/.
21. Lucy, Watts MBE, "HANs week, tube feeding, TPN and awareness," 2014, Available: http://www.lucy-watts.co.uk/2014/08/hans-week-tube-feeding-tpn-and-awareness.html.
22. Shukla, B. K., N. Kashyap, and R. K. Baghel, "Circular slotted elliptical patch antenna with elliptical notch in ground," *Progress In Electromagnetics Research C*, Vol. 74, 181–189, 2017.